# Surprising Quenching of the Spin−Orbit Interaction Significantly Diminishes H 2 O···X [X = F, Cl, Br, I] Dissociation Energies

**ARTICLE** *in* THE JOURNAL OF PHYSICAL CHEMISTRY A · AUGUST 2014

Impact Factor: 2.69 · DOI: 10.1021/jp506287z · Source: PubMed



**3 AUTHORS**, INCLUDING:

Gabor Czako
University of Szeged
**62** PUBLICATIONS **1,489** CITATIONS
SEE PROFILE

Attila Csaszar
Eötvös Loránd University
**197** PUBLICATIONS **5,725** CITATIONS
SEE PROFILE

THE JOURNAL OF PHYSICAL CHEMISTRY A

Article

pubs.acs.org/JPCA

# Surprising Quenching of the Spin−Orbit Interaction Significantly Diminishes $H_2O\cdots X$ [X = F, Cl, Br, I] Dissociation Energies

Gábor Czakó,*[,†] Attila G. Császár,*[,†,‡] and Henry F. Schaefer, III[§]

[†]Laboratory of Molecular Structure and Dynamics, Institute of Chemistry, Eötvös University, P.O. Box 32, H-1518 Budapest 112, Hungary

[‡]MTA-ELTE Research Group on Complex Chemical Systems, Pázmány Péter sétány 1/A, H-1117 Budapest, Hungary

[§]Center for Computational Quantum Chemistry, University of Georgia, Athens, Georgia 30602, United States

**ABSTRACT:** The $H_2O\cdots X$ complexes, with X = F, Cl, Br, and I, show considerable viability with nonspin−orbit $D_e(D_0)$ dissociation energy values of 3.73(2.42), 3.60(2.68), 3.54(2.72), and 3.36(2.77) kcal mol$^{-1}$ for X = F, Cl, Br, and I, respectively, obtained at the CCSD(T)-F12b/aug-cc-pVTZ(-PP) level of theory using relativistic pseudopotentials (PPs) for Br and I. Spin−orbit (SO) corrections, computed with the Breit−Pauli operator in the interacting states approach at the all-electron MRCI+Q/aug-cc-pwCVTZ(-PP) level, are found to depend sensitively and unpredictably on the O···X separations. 96% (F), 87% (Cl), 54% (Br), and 30% (I) quenching of the SO corrections significantly reduces the dissociation energies of the $H_2O\cdots X$ complexes, resulting in $D_e(D_0)$ values of 3.38(2.06), 2.86(1.94), 1.64(0.83), and 1.23(0.64) kcal mol$^{-1}$ for X = F, Cl, Br, and I, respectively.

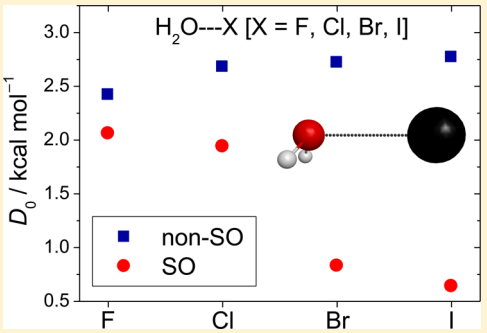


## I. INTRODUCTION

Although the reactions of halogen atoms with water have been of interest for quite some time,[1−3] new experiments[4] and sophisticated computations[5−14] reveal many important new features of these seemingly simple reactions. The recent $H_2O\cdots F^-$ photodetachment experiments of Continetti and co-workers[4] were combined with thorough theoretical analysis to provide a new picture for the dynamics of the prototypical F + $H_2O$ reaction.[4] Similar experiments would be valuable for the analogous Cl, Br, and I atom systems.

From a theoretical perspective, it is obvious that as one goes down the periodic table from F + $H_2O$ to I + $H_2O$, relativistic effects will become increasingly important. One feature of the related potential energy surfaces for which relativistic effects might seem unimportant is the dissociation energy for the entrance complexes $H_2O\cdots X$. In these complexes the distances between the halogen atom and the water molecule are substantial, and it is not unreasonable to assume that the magnitude of the spin−orbit (SO) interaction of the entrance complex is about the same as that of the isolated halogen atom.

However, recent computations by Bowman and co-workers[15] for the Br + $H_2O$ system point to a rather different interpretation. Because their interest was in the HBr + OH reaction, they paid little attention to the $H_2O\cdots$Br entrance well. Nevertheless, in a follow-up study of the same system, Zhang et al.[7] noted that Bowman's results indicate a significant quenching of the $H_2O\cdots$Br dissociation energy due to SO coupling. Zhang et al.[7] expressed some surprise that the large equilibrium separation between Br and $H_2O$ could alter the atomic SO coupling so much. In the present research, we address the dependence of the $H_2O\cdots X$ dissociation energies for all the halogen atoms, i.e., for X = F, Cl, Br, and I. Our results do confirm the work of Bowman and co-workers[15] qualitatively but contain some surprises for the other three systems.

## II. COMPUTATIONAL DETAILS

The electronic structure computations performed utilize the aug-cc-pVnZ [n = D, T, and Q] and aug-cc-pwCVnZ [n = D and T] correlation consistent basis set family of Dunning and co-workers[16] and small-core energy-consistent relativistic pseudopotentials (PPs) of the Stuttgart/Köln type[17] with the corresponding aug-cc-pVnZ-PP [n = D, T, and Q] and aug-cc-pwCVnZ-PP [n = D and T] basis sets[17] for Br and I. The PPs replace the inner-core electrons of Br ($1s^22s^22p^6$) and I ($1s^22s^22p^63s^23p^63d^{10}$), thereby accounting for the large scalar relativistic effects.

As to the level of electronic structure treatment, a variant of the restricted open-shell Hartree−Fock-based explicitly correlated unrestricted coupled cluster singles and doubles and perturbative triples method, ROHF-UCCSD(T)-F12b,[18] is employed for the geometry optimizations and harmonic frequency computations and a multiconfigurational self-consistent field (MCSCF) method, a corrected multireference configuration interaction [MRCI+Q][19,20] method, and an explicitly correlated MRCI+Q [MRCI-F12+Q] method are

**Special Issue:** David R. Yarkony Festschrift

**Received:** June 24, 2014
**Revised:** August 14, 2014
**Published:** August 18, 2014

   dx.doi.org/10.1021/jp506287z | J. Phys. Chem. A 2014, 118, 11956−11961

Table 1. Equilibrium Structures (in Å and degrees) and Non-SO and SO-Corrected $D_e$ and $D_0$ Values (in kcal mol$^{-1}$) for $H_2O\cdots X$ [X = F, Cl, Br, I]

| | non-SO (CCSD(T)-F12b)[a] | | | | | | | SO-corrected (AE-MRCI+Q)[b] | | | | |
|---|---|---|---|---|---|---|---|---|---|---|---|---|
| basis[c] | $R$(O···X) | $R$(OH) | $\alpha$(HOX) | $\tau$(HOXH) | $D_e$ | ΔZPE | $D_0$ | X + $H_2O$ | $H_2O\cdots X$ | ΔSO | $D_e$ | $D_0$ |
| | | | | | | $H_2O\cdots F$ | | | | | | |
| DZ | 2.114 | 0.963 | 85.35 | 105.28 | 4.04 | −1.23 | 2.81 | −0.35 | −0.01 | −0.34 | 3.71 | 2.48 |
| TZ | 2.107 | 0.962 | 85.73 | 105.18 | 3.73 | −1.31 | 2.42 | −0.37 | −0.01 | −0.36 | 3.38 | 2.06 |
| | | | | | | $H_2O\cdots Cl$ | | | | | | |
| DZ | 2.563 | 0.962 | 95.53 | 105.47 | 3.86 | −0.96 | 2.90 | −0.82 | −0.10 | −0.73 | 3.13 | 2.17 |
| TZ | 2.586 | 0.961 | 96.59 | 105.78 | 3.60 | −0.92 | 2.68 | −0.84 | −0.11 | −0.73 | 2.86 | 1.94 |
| | | | | | | $H_2O\cdots Br$ | | | | | | |
| DZ | 2.744 | 0.961 | 100.56 | 107.36 | 3.65 | −0.82 | 2.83 | −3.43 | −1.48 | −1.95 | 1.70 | 0.87 |
| TZ | 2.757 | 0.961 | 100.56 | 107.35 | 3.54 | −0.81 | 2.72 | −3.51 | −1.61 | −1.90 | 1.64 | 0.83 |
| | | | | | | $H_2O\cdots I$ | | | | | | |
| DZ | 2.968 | 0.961 | 105.91 | 110.90 | 3.45 | −0.72 | 2.73 | −6.89 | −4.61 | −2.29 | 1.16 | 0.44 |
| TZ | 2.985 | 0.960 | 105.91 | 110.89 | 3.36 | −0.59 | 2.77 | −7.11 | −4.98 | −2.13 | 1.23 | 0.64 |

[a]All the complexes have $C_s$ point-group symmetry. The ZPE corrections are based on harmonic frequencies obtained at the ROHF-UCCSD(T)-F12b/aug-cc-pVDZ(-PP) and ROHF-UCCSD(T)-F12b/aug-cc-pVTZ(-PP) levels of theory. [b]The SO corrections, defined as the difference between the SO and non-SO ground-state electronic energies, are obtained at the AE-MRCI+Q(5,3)/aug-cc-pwCVDZ(-PP) and AE-MRCI +Q(5,3)/aug-cc-pwCVTZ(-PP) levels of theory. X + $H_2O$ denotes the halogen atom SO corrections at large monomer separations, and $H_2O\cdots X$ denotes the entrance-complex SO corrections at the ROHF-UCCSD(T)-F12b/aug-cc-pVTZ(-PP) equilibrium geometries. [c]DZ and TZ denote aug-cc-pVDZ(-PP) and aug-cc-pVTZ(-PP), respectively, for the non-SO and aug-cc-pwCVDZ(-PP) and aug-cc-pwCVTZ(-PP), respectively, for the SO computations (PPs and the corresponding PP basis sets are used for Br and I).

used for the SO computations. The Davidson correction[21] (+Q) is used to estimate higher-order correlation energy effects. All the single-reference electronic structure computations employ the usual frozen-core (FC) approach, whereas both the FC and all-electron (AE) approaches are used for the multireference computations. Note that in the AE computations the outer-core electrons, i.e., ($1s^2$) for O and F, ($2s^22p^6$) for Cl, ($3s^23p^63d^{10}$) for Br, and ($4s^24p^64d^{10}$) for I, as well as the valence electrons are correlated. A minimal active space of 5 electrons in the three spatial $n$p-like orbitals, where $n$ = 2, 3, 4, and 5 for F, Cl, Br, and I, respectively, and a large full-valence active space of 15 electrons in 10 spatial orbitals are used for the multireference computations. The SO computations employ the Breit−Pauli operator in the interacting-states approach.[22] The SO eigenstates are obtained by diagonalizing a 6 × 6 SO matrix, whose diagonal elements are replaced by the Davidson-corrected MRCI or MRCI-F12 energies, except for MCSCF. All the electronic structure computations are performed with the help of the *ab initio* program package MOLPRO.[23]

## III. RESULTS AND DISCUSSION

Structural parameters and non-SO and SO dissociation energies (both $D_e$ and $D_0$) of the $H_2O\cdots X$ [X = F, Cl, Br, I] complexes are reported in Table 1. The CCSD(T)-F12b method converges remarkably well with respect to basis size: the aug-cc-pVDZ and aug-cc-pVTZ Born−Oppenheimer equilibrium geometry parameter estimates agree within 0.001 Å for the intramolecular OH bond length and within about 0.02 Å for the more sensitive intermolecular O···X distances. The dissociation energies decrease by only about 0.1−0.3 kcal mol$^{-1}$ if the basis is increased from DZ to TZ. Thus, knowing the fast convergence of the F12 methods, we can be confident that the aug-cc-pVTZ relative energies are converged to within about 0.1 kcal mol$^{-1}$. The post-CCSD(T) electron correlation effect, the core−valence correlation effect, and the scalar relativistic effect on H, O, F, and Cl and the error of the PP approximation for Br and I are expected to be small. For example, it is stated in ref 15 that the above auxiliary corrections for $H_2O\cdots Br$ are 0.02, 0.08, and 0.00 kcal/mol, respectively. Note that the use of PP accounts for the scalar relativistic effect on Br; thus, the 0.00 kcal/mol correction corresponds to the scalar relativistic effect on H and O and the inaccuracy of the PP approximation.[15]

The equilibrium O···X distances are 2.107, 2.586, 2.757, and 2.985 Å for X = F, Cl, Br, and I, respectively, and the corresponding $D_e$ values without SO coupling are in the same ballpark at 3.73, 3.60, 3.54, and 3.36 kcal mol$^{-1}$. For X = F and Cl the present $D_e$ values agree with those of Guo and co-workers,[14] as they used the same level of electronic structure theory. For X = Br, Guo and co-workers[14] reported a slightly different $D_e$ of 3.47 kcal mol$^{-1}$, because they did not employ a pseudopotential for Br. Here a $D_e$ of 3.54 kcal mol$^{-1}$ has been obtained with PP and the corresponding aug-cc-pVTZ-PP basis set. As seen, the O···X equilibrium distances increase and the $D_e$ values slightly decrease as we go from X = F to X = I. As the binding gets looser, the harmonic zero-point vibrational energies (ZPEs) of the $H_2O\cdots X$ complexes decrease, the ZPEs are 5172, 5035, 4997, and 4920 cm$^{-1}$ for X = F, Cl, Br, and I, respectively, whereas the ZPE of $H_2O$ is 4713 cm$^{-1}$. As a result, the ZPE corrections significantly decrease the dissociation energies, for $H_2O\cdots F$ by 1.31 kcal mol$^{-1}$ and the absolute ZPE effects become smaller and smaller: 0.92, 0.81, and 0.59 kcal mol$^{-1}$ for X = Cl, Br, and I, in order. Therefore, the ZPE corrections reverse the order of the dissociation energies. In other words, unlike the $D_e$ values, the $D_0$ values slightly increase from X = F to I, they are 2.42, 2.68, 2.72, and 2.77 kcal mol$^{-1}$ for X = F, Cl, Br, and I, respectively. At this point, the present $D_e$ and $D_0$ values agree well with previous theoretical predictions.[5−8,14] However, most of the previous studies did not consider the SO effects on the dissociation energies.

To understand the SO effects on the dissociation energies of the $H_2O\cdots X$ [X = F, Cl, Br, I] complexes, we computed one-dimensional non-SO and SO potential energy curves as a function of the O···X distance, maintaining the $C_s$ point-group symmetry and keeping the other internal coordinates ($R_{OH}$,


dx.doi.org/10.1021/jp506287z | J. Phys. Chem. A 2014, 118, 11956−11961

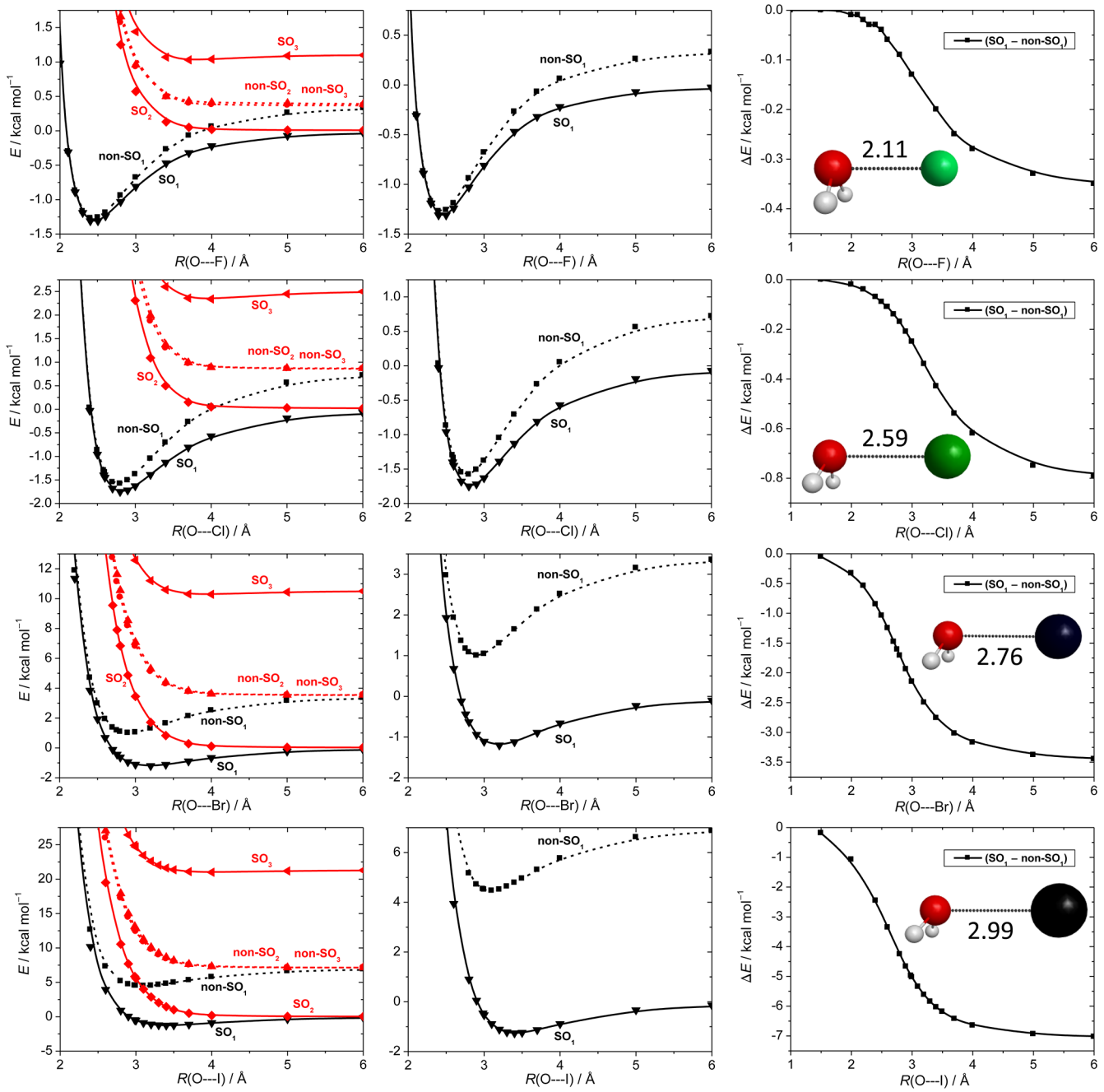


**Figure 1.** Potential energy curves obtained at the AE-MRCI+Q(5,3)/aug-cc-pwCVTZ(-PP) (PPs for Br and I) level as a function of the $H_2O\cdots X$ [X = F, Cl, Br, I] separation, keeping the $H_2O$ unit at the CCSD(T)-F12b/aug-cc-pVTZ(-PP) equilibrium structure corresponding to the entrance-channel complex ($C_s$). $SO_1$ and non-$SO_1$ (black curves) denote the spin−orbit (SO) and non-SO ground electronic states, respectively, whereas the red curves correspond to excited states. In the right panels the energy differences between the SO and non-SO ground states are shown as a function of the O···X distance.

$\alpha_{HOX}$, $\tau_{HOXH}$) fixed at their equilibrium values corresponding to the $H_2O\cdots X$ minima. Figure 1 shows the potentials for the non-SO ground electronic state and the two quasi-degenerate excited electronic states, which are not reactive within an adiabatic approximation. All three non-SO states correlate with the $X(^2P) + H_2O$ asymptote. The SO coupling splits the ground state of the X atom ($^2P$) to a 4-fold degenerate SO ground state ($^2P_{3/2}$) and a 2-fold degenerate SO excited state ($^2P_{1/2}$). As X approaches $H_2O$, the 4-fold degenerate state splits into two doubly degenerate SO states (Figure 1, left panels).

As seen in Figure 1 (middle panels), the non-SO and SO-corrected ground-state potentials approach each other as the O···X distance decreases and the two curves merge at an O···X separation around 1.5−2.5 Å. Our interest is in the energy difference between the SO and non-SO ground electronic states, $\Delta E_{SO} = E_{SO} - E_{non\text{-}SO}$, because the $\Delta E_{SO}(X) - \Delta E_{SO}(H_2O\cdots X)$ values are the SO corrections for the dissociation energies. As Figure 1 (right panels) shows, the SO corrections depend very sensitively on the O···X separations. The absolute $\Delta E_{SO}$ decreases steeply, especially between O···X distances of 4 and 2 Å, as X approaches $H_2O$,


dx.doi.org/10.1021/jp506287z | J. Phys. Chem. A 2014, 118, 11956−11961

Table 2. Spin−Orbit Corrections (in kcal mol$^{-1}$) at Different Levels of Theory for X + $H_2O$ and $H_2O$···X [X = F, Cl, Br, I][a]

| level of theory[b] | F + $H_2O$ | $H_2O$···F | ΔSO | Cl + $H_2O$ | $H_2O$···Cl | ΔSO | Br + $H_2O$ | $H_2O$···Br | ΔSO | I + $H_2O$ | $H_2O$···I | ΔSO |
|---|---|---|---|---|---|---|---|---|---|---|---|---|
| MCSCF(5,3)/aVDZ | −0.36 | −0.02 | −0.34 | −0.78 | −0.09 | −0.69 | −3.35 | −1.45 | −1.90 | −6.94 | −4.63 | −2.31 |
| MCSCF(5,3)/aVTZ | −0.37 | −0.02 | −0.35 | −0.78 | −0.10 | −0.68 | −3.35 | −1.50 | −1.86 | −6.92 | −4.71 | −2.21 |
| MCSCF(5,3)/aVQZ | −0.38 | −0.02 | −0.36 | −0.78 | −0.10 | −0.69 | −3.36 | −1.50 | −1.86 | −6.93 | −4.73 | −2.20 |
| MCSCF(15,10)/aVDZ | −0.36 | −0.02 | −0.34 | −0.78 | −0.08 | −0.70 | −3.35 | −1.37 | −1.98 | −6.94 | −4.50 | −2.44 |
| MCSCF(15,10)/aVTZ | −0.37 | −0.02 | −0.35 | −0.78 | −0.09 | −0.69 | −3.35 | −1.40 | −1.95 | −6.92 | −4.57 | −2.35 |
| MRCI+Q(5,3)/aVDZ | −0.34 | −0.01 | −0.33 | −0.75 | −0.08 | −0.67 | −3.22 | −1.29 | −1.93 | −6.66 | −4.33 | −2.32 |
| MRCI+Q(5,3)/aVTZ | −0.37 | −0.01 | −0.35 | −0.76 | −0.08 | −0.68 | −3.25 | −1.39 | −1.86 | −6.67 | −4.52 | −2.15 |
| MRCI+Q(5,3)/aVQZ | −0.38 | −0.01 | −0.36 | −0.76 | −0.08 | −0.68 | −3.27 | −1.40 | −1.87 | −6.73 | −4.56 | −2.16 |
| MRCI+Q(15,10)/aVDZ | −0.34 | −0.01 | −0.33 | −0.76 | −0.07 | −0.69 | −3.28 | −1.28 | −2.00 | −6.76 | −4.33 | −2.43 |
| MRCI+Q(15,10)/aVTZ | −0.37 | −0.01 | −0.36 | −0.77 | −0.08 | −0.69 | −3.30 | −1.36 | −1.94 | −6.78 | −4.50 | −2.28 |
| MRCI-F12+Q(5,3)/aVDZ | −0.35 | −0.01 | −0.34 | −0.76 | −0.08 | −0.68 | −3.29 | −1.40 | −1.88 | −6.80 | −4.63 | −2.17 |
| MRCI-F12+Q(5,3)/aVTZ | −0.37 | −0.01 | −0.35 | −0.76 | −0.09 | −0.68 | −3.27 | −1.40 | −1.87 | −6.72 | −4.55 | −2.17 |
| MRCI-F12+Q(5,3)/aVQZ | −0.38 | −0.01 | −0.36 | −0.77 | −0.09 | −0.68 | −3.28 | −1.40 | −1.88 | −6.74 | −4.57 | −2.17 |
| MRCI-F12+Q(15,10)/aVDZ | −0.35 | −0.01 | −0.34 | −0.77 | −0.08 | −0.69 | −3.31 | −1.38 | −1.94 | −6.84 | −4.60 | −2.24 |
| MRCI-F12+Q(15,10)/aVTZ | −0.37 | −0.01 | −0.36 | −0.77 | −0.08 | −0.69 | −3.31 | −1.37 | −1.94 | −6.81 | −4.53 | −2.28 |
| AE-MRCI+Q(5,3)/awCVDZ | −0.35 | −0.01 | −0.34 | −0.82 | −0.10 | −0.73 | −3.43 | −1.48 | −1.95 | −6.89 | −4.61 | −2.29 |
| AE-MRCI+Q(5,3)/awCVTZ | −0.37 | −0.01 | −0.36 | −0.84 | −0.11 | −0.73 | −3.51 | −1.61 | −1.90 | −7.11 | −4.98 | −2.13 |
| experiment[c] | −0.39 | | | −0.84 | | | −3.51 | | | −7.25 | | |

[a]The SO corrections are defined as the difference between the SO and non-SO ground-state electronic energies, $E_{SO} - E_{non\text{-}SO}$. F, Cl, Br, and I + $H_2O$ denote the SO corrections for the corresponding F, Cl, Br, and I + $H_2O$ asymptotic limits and $H_2O$···F, $H_2O$···Cl, $H_2O$···Br, and $H_2O$···I denote the entrance-complex SO corrections at the ROHF-UCCSD(T)-F12b/aug-cc-pVTZ(-PP) equilibrium geometries. ΔSO denotes the SO corrections for the dissociation energies. [b]aVDZ, aVTZ, and aVQZ denote the corresponding aug-cc-pVnZ(-PP) [n = D, T, and Q] bases and awCVDZ and awCVTZ denote the corresponding aug-cc-pwCVnZ(-PP) [n = D and T] basis sets. PPs and the corresponding PP basis sets are used for Br and I. (5,3) and (15,10) denote active spaces of 5 electrons in 3 orbitals and 15 electrons in 10 orbitals, respectively. For further details see text. [c]Experimental data are obtained from the measured atomic SO splittings of $\varepsilon$ = 1.16(F), 2.52(Cl), 10.54(Br), and 21.74(I) kcal mol$^{-1}$, as $-\varepsilon/3$.[30]

and almost completely quenches at a 1.5 Å O···X separation. Because the equilibrium O···X distances of the $H_2O$···X complexes are in the 2−3 Å range, the $\Delta E_{SO}(H_2O\cdots X)$ corrections are not equal to the $\Delta E_{SO}(X)$ values for the X + $H_2O$ asymptotic limits; thus, significant SO effects on the dissociation energies are expected. In the cases of $H_2O$···F and $H_2O$···Cl, which have the shortest O···X equilibrium distances of 2.11 and 2.59 Å, respectively, the $\Delta E_{SO}$ corrections are almost completely quenched (−0.01 and −0.11 kcal mol$^{-1}$, respectively). Thus, the corresponding dissociation energies are lowered by 0.36 and 0.73 kcal mol$^{-1}$, these values are almost equal to the atomic SO corrections. For $H_2O$···Br the quenching of $\Delta E_{SO}$ is also substantial, because $\Delta E_{SO}(H_2O\cdots Br)$ = −1.61 kcal mol$^{-1}$, whereas $\Delta E_{SO}(Br)$ = −3.51 kcal mol$^{-1}$; thus, the dissociation energy is significantly reduced by 1.90 kcal mol$^{-1}$. As expected, the O···X separation is the largest in $H_2O$···I (2.99 Å), but even at this large distance $\Delta E_{SO}$ is −4.98 kcal mol$^{-1}$. As the atomic correction is −7.11 kcal mol$^{-1}$, there is a large decrease of the dissociation energy by 2.13 kcal mol$^{-1}$.

We have investigated the dependence of the above-described SO corrections upon the level of electronic structure theory, shown in Table 2. A TZ basis with a minimal active space provides reasonably accurate results, because the aug-cc-pVTZ and aug-cc-pVQZ SO corrections agree within 0.06 kcal mol$^{-1}$ (or even better with F12) and the minimal and full-valence active spaces give the same results within 0.12 kcal mol$^{-1}$. A more significant effect is found when we correlate the core electrons, especially for X = Br and I, where the $\Delta E_{SO}(X)$ values change by 0.26 and 0.44 kcal mol$^{-1}$, respectively, thereby improving the agreement with experiment, as shown in Table 2. It is important to note that if we consider the $\Delta E_{SO}(X) - \Delta E_{SO}(H_2O\cdots X)$ corrections, which are the real interest of the present study, the core-correlation effects are less than 0.06 kcal mol$^{-1}$ for all cases. Because the all-electron results give the best agreement with the measured atomic SO splittings, we use the AE-MRCI+Q(5,3)/aug-cc-pwCVTZ SO corrections to compute the final estimates for the dissociation energies.

Applying the SO corrections to the dissociation energies, we get $D_e$ values of 3.38, 2.86, 1.64, and 1.23 kcal mol$^{-1}$ for $H_2O$···X with X = F, Cl, Br, and I, respectively, whereas the corresponding $D_0$ values are reduced to 2.06, 1.94, 0.83, and 0.64 kcal mol$^{-1}$, in order. Clearly, the SO corrections substantially reduce the dissociation energies. Even if the quenching of $\Delta E_{SO}$ is most significant for the complex $H_2O$···F, the SO correction has the largest effect on the dissociation energy of $H_2O$···I, because the SO splitting of iodine is an order of magnitude larger than that of fluorine. For $H_2O$···Br the present SO-corrected $D_e$ value of 1.64 kcal mol$^{-1}$ confirms the recent prediction of Bowman and co-workers,[15] 1.62 kcal mol$^{-1}$.

Because the magnitude of the SO correction depends sensitively on the O···X separation, the SO coupling affects the position of the minima (Figure 1). This geometry effect is negligible for X = F and Cl, but substantial (about +0.3 Å) for X = Br and I, as seen in Figure 1 (middle panels). Note also that MRCI+Q overestimates the CCSD(T)-F12b equilibrium O···X distances by about 0.1−0.2 Å if a minimal active space is employed for MRCI, because CCSD(T)-F12b provides a much more accurate description of the dynamical electron correlation. If we use the large full-valence active space, MRCI+Q reproduces well the CCSD(T) geometries for X = Cl, Br, and I, indicating that static electron correlation is not significant at the $H_2O$···X minima, except for $H_2O$···F. The $T_1$ diagnostic[24] further supports the above findings, because $T_1$ = 0.033 for $H_2O$···F, whereas for X = Cl, Br, and I the $T_1$ diagnostic values of 0.017, 0.013, and 0.010, respectively, are well below 0.02, indicating that single-reference correlation methods can describe the $H_2O$···X [X = Cl, Br, and I] complexes well.


dx.doi.org/10.1021/jp506287z | J. Phys. Chem. A 2014, 118, 11956−11961

Due to the large dipole moment of $H_2O$ and the covalent nature of the O···X bond,[14] the $H_2O$···X complexes are expected to be much more stable than the corresponding $CH_4$···X complexes. In the case of the $CH_4$···X complexes the shallower minima correspond to single-H-bonded $H_3CH$···X ($C_{3v}$) structures and deeper minima were found at the $HCH_3$···X ($C_{3v}$) arrangements.[25−29] Without SO corrections the $D_e$ values for the $H_3CH$···X complexes are about 0.3 kcal mol$^{-1}$, whereas $HCH_3$···X have $D_e$ of about 0.9 kcal mol$^{-1}$.[25−29] These $D_e$ values are indeed much smaller than the corresponding $H_2O$···X dissociation energies. However, due to the much larger C···X separations at $H_3CH$···X ($R_{CX}$ = 3.5−4.5 Å) as compared to the corresponding O···X distances ($R_{OX}$ = 2.0−3.0 Å), the SO effects are negligible for the dissociation energies of $H_3CH$···X.[25−29] For $HCH_3$···X, where the C···X distances are in the range 3.0−4.0 Å, the SO corrections are slightly quenched, thereby decreasing the dissociation energies by about 0.3 kcal mol$^{-1}$, resulting in $D_e$ values of about 0.6 kcal mol$^{-1}$.[25−28] Thus, for X = F and Cl the $H_2O$···X complexes are indeed much more strongly bound than the corresponding $CH_4$···X complexes. However, for X = Br and I, where the large quenching of the SO corrections significantly diminishes the $H_2O$···X dissociation energies, the $H_2O$···X and $CH_4$···X complexes have comparable dissociation energies.

## IV. SUMMARY AND CONCLUSIONS

Several dynamical studies have shown that entrance-channel complexes may play important steering roles in the dynamics of bimolecular chemical reactions, thereby influencing the outcome of the reactions.[9,26] $H_2O$ forms promising complexes with halogen atoms F, Cl, Br, and I, whereby the $D_e$ and $D_0$ values vary in the ranges of 3.3−3.8 and 2.4−2.8 kcal mol$^{-1}$, respectively, if SO interactions are not considered. It is well-known that SO coupling lowers the reactant asymptote of the X + $H_2O$ reactions by the SO correction of the halogen atom. For an entrance-channel complex, one may expect that the SO correction at the geometry of the complex is the same as the atomic limit; thus, there may be no effect on the dissociation energy. The present study shows, however, that 96, 87, 54, and 30% of the atomic SO corrections, defined as $E_{SO} - E_{non\text{-}SO}$, are quenched for the $H_2O$···X complexes, where X = F, Cl, Br, and I, respectively, thereby reducing the dissociation energies by 0.36, 0.73, 1.90, and 2.13 kcal mol$^{-1}$, in order. (Note that unlike $E_{SO} - E_{non\text{-}SO}$, the measurable SO splittings between the lowest and highest SO states, defined as $E_{SO}$(excited) − $E_{SO}$(ground), increase as X approaches $H_2O$.) Though the percentagewise quenching of ($E_{SO} - E_{non\text{-}SO}$) is getting smaller from X = F to I, the SO effects on the dissociation energies are more and more substantial if we go down the periodic table, because the atomic SO corrections increase rapidly from F to I. Whereas the non-SO $D_0$ values are similar for all the $H_2O$···X complexes, the SO-corrected $D_0$ values are 2.06, 1.94, 0.83, and 0.64 kcal mol$^{-1}$ for X = F, Cl, Br, and I, respectively.

## AUTHOR INFORMATION


### Corresponding Authors

*G. Czakó. E-mail: czako@chem.elte.hu.

*A. G. Császár. E-mail: csaszar@chem.elte.hu.


### Notes

The authors declare no competing financial interest.

## ACKNOWLEDGMENTS

G.C. and A.G.C. were supported by the Scientific Research Fund of Hungary (OTKA, NK83583). H.F.S. thanks the U.S. Department of Energy, Office of Basic Energy Sciences, Chemistry Division for support.

## REFERENCES


(1) Ziemkiewicz, M.; Wojcik, M.; Nesbitt, D. J. Direct Evidence for Nonadiabatic Dynamics in Atom + Polyatom Reactions: Crossed-Jet Laser Studies of F + $D_2O$ → DF + OD. *J. Chem. Phys.* **2005**, *123*, 224307.

(2) Sinha, A.; Thoemke, J. D.; Crim, F. F. Controlling Bimolecular Reactions: Mode and Bond Selected Reaction of Water with Translationally Excited Chlorine Atoms. *J. Chem. Phys.* **1992**, *96*, 372−376.

(3) Nyman, G.; Clary, D. C. Vibrational and Rotational Effects in the Cl + HOD ↔ HCl + OD Reaction. *J. Chem. Phys.* **1994**, *100*, 3556−3567.

(4) Otto, R.; Ma, J.; Ray, A. M.; Daluz, J. S.; Li, J.; Guo, H.; Continetti, R. E. Imaging Dynamics on the F + $H_2O$ → HF + OH Potential Energy Surfaces from Wells to Barriers. *Science* **2014**, *343*, 396−399.

(5) Li, G.; Zhou, L.; Li, Q.-S.; Xie, Y.; Schaefer, H. F. The Entrance Complex, Transition State, and Exit Complex for the F + $H_2O$ → HF + OH Reaction. Definitive Predictions. Comparison with Popular Density Functional Methods. *Phys. Chem. Chem. Phys.* **2012**, *14*, 10891−10895.

(6) Guo, Y.; Zhang, M.; Xie, Y.; Schaefer, H. F. Communication: Some Critical Features of the Potential Energy Surface for the Cl + $H_2O$ → HCl + OH Forward and Reverse Reactions. *J. Chem. Phys.* **2013**, *139*, 041101.

(7) Zhang, M.; Hao, Y.; Guo, Y.; Xie, Y.; Schaefer, H. F. Anchoring the Potential Energy Surface for the Br + $H_2O$ → HBr + OH Reaction. *Theor. Chem. Acc.* **2014**, *133*, 1513−1521.

(8) Hao, Y.; Gu, J.; Guo, Y.; Zhang, M.; Xie, Y.; Schaefer, H. F. Spin-Orbit Corrected Potential Energy Surface Features for the I($^2P_{3/2}$) + $H_2O$ → HI + OH Forward and Reverse Reactions. *Phys. Chem. Chem. Phys.* **2014**, *16*, 2641−2646.

(9) Li, J.; Jiang, B.; Guo, H. Enhancement of Bimolecular Reactivity by a Pre-Reaction van der Waals Complex: the case of F + $H_2O$ → HF + HO. *Chem. Sci.* **2013**, *4*, 629−632.

(10) Li, J.; Dawes, R.; Guo, H. An Ab Initio Based Full-Dimensional Global Potential Energy Surface for $FH_2O(X^2A')$ and Dynamics for the F + $H_2O$ → HF + HO Reaction. *J. Chem. Phys.* **2012**, *137*, 094304.

(11) Li, J.; Jiang, B.; Guo, H. Spin-Orbit Corrected Full-Dimensional Potential Energy Surfaces for the Two Lowest-Lying Electronic States of $FH_2O$ and Dynamics for the F + $H_2O$ → HF + OH Reaction. *J. Chem. Phys.* **2013**, *138*, 074309.

(12) Nguyen, T. L.; Li, J.; Dawes, R.; Stanton, J. F.; Guo, H. Accurate Determination of Barrier Height and Kinetics for the F + $H_2O$ → HF + OH Reaction. *J. Phys. Chem. A* **2013**, *117*, 8864−8872.

(13) Li, J.; Dawes, R.; Guo, H. Kinetic and Dynamic Studies of the Cl($^2P_u$) + $H_2O(X^1A_1)$ → HCl($X^1\Sigma^+$) + OH($X^2\Pi$) Raction on an Ab Initio Based Full-Dimensional Global Potential Energy Surface of the Ground Electronic State of $ClH_2O$. *J. Chem. Phys.* **2013**, *139*, 074302.

(14) Li, J.; Li, Y.; Guo, H. Communication: Covalent Nature of X···$H_2O$ (X = F, Cl, and Br) Interactions. *J. Chem. Phys.* **2013**, *138*, 141102.

(15) de Oliveira-Filho, A. G. S.; Ornellas, F. R.; Bowman, J. M. Quasiclassical Trajectory Calculations of the Rate Constant of the OH + HBr → Br + $H_2O$ Reaction Using a Full-Dimensional Ab Initio Potential Energy Surface Over the Temperature Range 5 to 500 K. *J. Phys. Chem. Lett.* **2014**, *5*, 706−712.

(16) Dunning, T. H., Jr. Gaussian Basis Sets for Use in Correlated Molecular Calculations. I. The Atoms Boron Through Neon and Hydrogen. *J. Chem. Phys.* **1989**, *90*, 1007−1023.

(17) Peterson, K. A.; Figgen, D.; Goll, E.; Stoll, H.; Dolg, M. Systematically Convergent Basis Sets with Relativistic Pseudopoten-

tials. II. Small-Core Pseudopotentials and Correlation Consistent Basis Sets for the Post-*d* Group 16−18 Elements. *J. Chem. Phys.* **2003**, *119*, 11113−11123.
(18) Knizia, G.; Adler, T. B.; Werner, H.-J. Simplified CCSD(T)-F12 Methods: Theory and Benchmarks. *J. Chem. Phys.* **2009**, *130*, 054104.
(19) Werner, H.-J.; Knowles, P. J. An Efficient Internally Contracted Multiconfiguration-Reference Configuration Interaction Method. *J. Chem. Phys.* **1988**, *89*, 5803−5814.
(20) Knowles, P. J.; Werner, H.-J. An Efficient Method for the Evaluation of Coupling Coefficients in Configuration Interaction Calculations. *Chem. Phys. Lett.* **1988**, *145*, 514−522.
(21) Langhoff, S. R.; Davidson, E. R. Configuration Interaction Calculations on the Nitrogen Molecule. *Int. J. Quantum Chem.* **1974**, *8*, 61−72.
(22) Berning, A.; Schweizer, M.; Werner, H.-J.; Knowles, P. J.; Palmieri, P. Spin-Orbit Matrix Elements for Internally Contracted Multireference Configuration Interaction Wavefunctions. *Mol. Phys.* **2000**, *98*, 1823−1833.
(23) Werner, H.-J.; Knowles, P. J.; Knizia, G.; Manby, F. R.; Schütz, M.; et al. *Molpro*, version 2012.1, a package of ab initio programs; http://www.molpro.net.
(24) Lee, T. J.; Taylor, P. R. A Diagnostic for Determining the Quality of Single-Reference Electron Correlation Methods. *Int. J. Quantum Chem.* **1989**, *S23*, 199−207.
(25) Czakó, G.; Bowman, J. M. An Ab Initio Spin−Orbit-Corrected Potential Energy Surface and Dynamics for the F + $CH_4$ and F + $CHD_3$ Reactions. *Phys. Chem. Chem. Phys.* **2011**, *13*, 8306−8312.
(26) Czakó, G.; Bowman, J. M. Dynamics of the Reaction of Methane with Chlorine Atom on an Accurate Potential Energy Surface. *Science* **2011**, *334*, 343−346.
(27) Czakó, G.; Bowman, J. M. Accurate Ab Initio Potential Energy Surface, Thermochemistry, and Dynamics of the Cl($^2$P, $^2P_{3/2}$) + $CH_4$ → HCl + $CH_3$ and H + $CH_3$Cl Reactions. *J. Chem. Phys.* **2012**, *136*, 044307.
(28) Czakó, G. Accurate Ab Initio Potential Energy Surface, Thermochemistry, and Dynamics of the Br($^2$P, $^2P_{3/2}$) + $CH_4$ → HBr + $CH_3$ Reaction. *J. Chem. Phys.* **2013**, *138*, 134301.
(29) Cheng, M.; Feng, Y.; Du, Y.; Zhu, Q.; Zheng, W.; Czakó, G.; Bowman, J. M. Communication: Probing the Entrance Channels of the X + $CH_4$ → HX + $CH_3$ (X = F, Cl, Br, I) Reactions Via Photodetachment of $X^-$−$CH_4$. *J. Chem. Phys.* **2011**, *134*, 191102.
(30) The National Institute of Standards and Technology (NIST), *Handbook of Basic Atomic Spectroscopic Data*, http://www.nist.gov/pml/data/handbook/.